Journal of Inorganic Biochemistry 191 (2019) 135–142

Contents lists available at ScienceDirect

Journal of Inorganic Biochemistry

journal homepage: www.elsevier.com/locate/jinorgbio

Engineering of pectin-dopamine nano-conjugates for carrying ruthenium complex: A potential tool for biomedical applications

Jiajing Diao[a,1], Feng Bai[a,c,1], Ying Wang[a,c], Qianqian Han[a,c], Xi Xu[b,*], Hongmei Zhang[a,*], Qiang Luo[a,c], Yanqing Wang[a,*]

[a] Institute of Environmental Toxicology and Environmental Ecology, Yancheng Teachers University, Yancheng City, Jiangsu Province 224007, People's Republic of China
[b] Center for Molecular Metabolism, Nanjing University of Science & Technology, B508, No. 364 Building, 200 Xiaolinwei Street, Nanjing 210094, People's Republic of China
[c] Chemistry and Chemical Engineering, Nanjing University of Technology, Nanjing City, Jiangsu Province 210009, People's Republic of China

ARTICLE INFO

Keywords:
Pectin
Dopamine
Ruthenium complex
Nano-conjugates
Anticancer activity

ABSTRACT

In this work, we designed polysaccharide-metal complex of dopamine-modified pectin linking ruthenium compound, which exhibited a certain inhibition specificity to human renal cell adenocarcinoma cell line 786-O. The chemical structure and physical properties of the polysaccharide-metal complex were well characterized by multiple analysis methods. The multi-spectral results revealed that pectin-dopamine have been successfully coordinated by ruthenium complex to form nano-conjugates, which self-assembled into relatively regular nanospheres of approximately 200 nm. The polysaccharide-metal complex has more amorphous and less viscosity than pectin, and cannot withstand as much strain as the pectin and pectin-dopamine systems. Pectin-dopamine can decrease the toxicity effect of Ru complex in normal cell line such as human normal renal epithelial cell line 293A.

1. Introduction

For the past few years, the development of new polymer-metal complexes (PMCs) was the new research for cancer therapies. The polymers with the biocompatible and biodegradable properties acted as skeleton material of PMCs by associating with platinum and ruthenium complexes have been approved for treatment of cancer [1–3]. For example, Valente et al. have synthesized D -glucose end-capped polylactide ruthenium cyclopentadienyl complex (RuPMC), which has potential application of RuPMC as a new drug delivery system [3]. Based on the chemical structures of PMCs in aqueous solutions, they can self-assemble into different nanostructures [4]. Many kinds of nanostructures carrying anticancer drug have been designed to decrease related side effects and further improve their use in cancer treatment [5–7]. In the construction of nanoscale drug carrying materials, some natural multifunctional drug carriers such as albumin, lipoproteins and polysaccharides have been extensively studied for a number of biomedical and pharmaceutical applications [8–10]. Among them, natural occurring polysaccharides are the most popular biopolymeric materials due to their immunomodulatory, anti-inflammatory, and antitumor effects [11,12].

Pectin (PEC) is a polysaccharide consisting of linear chains of α-(1–4)-linked D-galacturonic acid residues, occasionally interrupted by α-(1–2)-linked L-rhamnose [13]. Recent, Lei et al. have designed a natural PEC nano-platform for delivery of two anticancer drugs, which has a promising potential for anti-cancer combination therapy [14]. Sriamornsak et al. have synthesized thiolated pectin–doxorubicin conjugates that might be suitable for building drug platform for colorectal cancer-targeted delivery of doxorubicin [13]. Vaidya et al. have engineered pectin-cisplatin nano-conjugates to enhance blood circulating levels of cisplatin in mice [15]. To the best of our knowledge, the development of nanostructured pectin carrying with anticancer metallodrugs is currently drawing attention with preparing satisfactory PEC-based nanoparticles. There have been no studies done on pectin-ruthenium conjugates using small active molecules bond linkage.

In this work, PEC was used as the polymer backbone modified by dopamine (DO) to coordinate ruthenium complex. DO, a catecholamine neurotransmitter, played a key role in transmission in the nervous, hormonal, cardiovascular, and renal systems. Alginate-linked DO can significantly increase the adhesion of biomaterials to intestinal tissue [16]. Due to the unique molecular structure of DO and its special properties such as strong anti-oxidant and coordination properties [17],

* Corresponding authors.
E-mail addresses: xuxi@njust.edu.cn (X. Xu), hxzhm@126.com (H. Zhang), wyqing76@126.com (Y. Wang).
[1] Jiajing Diao and Feng Bai contributed equally.

https://doi.org/10.1016/j.jinorgbio.2018.11.016
Received 27 August 2018; Received in revised form 22 November 2018; Accepted 25 November 2018
Available online 28 November 2018
0162-0134/

we have used it as a bridge to link PEC and ruthenium complex that have attracted wide attention as a model of metal-based anticancer drugs. Because of their low toxicity, ruthenium complexes have broad application prospect in anticancer [3,18,19,21,22]. The development of nanostructured materials functionalised with ruthenium complexes as alternatives for administering anticancer metallodrugs is currently receiving attention with natural polymers [1023–26, 28–30]. The polysaccharide-metal complex formed involving DO-modified PEC and a cis-Bis (2,2′-Dipyridyl) ruthenium (II) dichloride (Ru) were synthesized and characterized. In addition, the antioxidant activity, rheological property, and anti-cancer activity of PEC-DO + Ru conjugates were also studied in this work.

2. Materials and methods

2.1. Materials

Pectin (MW, 200 kDa, galacturonic acid, ≥77.4%), *cis*-Bis (2,2′-Dipyridyl) ruthenium(II) dichloride(~99%), dopamine hydrochloride (~99%), *N*-Hydroxy-succinimide (NHS, ~98%), *N*-(3-Dimethylaminopropyl)-*N*′-ethylcarbodiimide hydrochloride (EDC, ~98%), 2,2′-Azino-di-[3-ethylbenzthiazoline sulfonate] (ABTS), and 1,1-Diphenyl-2-picrylhydrazyl radical 2,2-Diphenyl-1-(2,4,6-trinitrophenyl) hydrazyl (DPPH) were all purchased from Aladdin (Shanghai PR China). All other chemicals were analytical grade and used as received.

2.2. Synthesis of PEC-DO conjugates

In a 500 mL glass flask, 2-(*N*-morpholine) ethanesulfonic acid (MES) (2.7 g) was dissolved in 500 mL of distilled water to prepare pH = 5.0 MES buffer. PEC (500 mg) was dissolved in 300 mL of MES buffer, which followed by the addition of an amount of 1:1 EDC and NHS as a coupling agent, and PEC was coupled to DO through the active ester intermediate. DO was dissolved in the MES buffer solution and the activated PEC was mixed with the DO solution. The mixture was stirred for 48 h under a nitrogen atmosphere and protected from light. After the reaction was over, the mixture was taken out into a dialysis bag, dialyzed with deionized water for four days, changed every 12 h, and finally lyophilized. Fig. 1(A) shows the synthetic route of PEC-DO conjugates.

2.3. Coordination of pectin-dopamine with cis-Bis(2,2′-Dipyridyl) ruthenium (II) dichloride

20 mg of *cis*-bis(2,2′-dipyridyl) ruthenium (II) chloride was dissolved in 5 mL of *N*,*N*-dimethyllformamide (DMF), < 1:1 M amount of silver nitrate was added, and a small amount of nitric acid was added, dropwise. The reaction was completed after 24 h. Then, the solution was centrifuged and the filtrate was obtained. 200 mg of PEC-DO conjugates was dissolved in 200 mL of deionized water, and the above filtrate was poured into a pectin-dopamine solution, protected from light for 24 h, and dialyzed against deionized water for four days (MWCO: 3500 Da). Finally, the solution was lyophilized to obtain a PEC-DO product carrying *cis*-bis(2,2′-dipyridyl) hafnium dichloride (II) (PEC-DO + Ru) and finally was stored frozen. Fig. 1(B) showed the preparation route of PEC-DO + Ru conjugates.

2.4. Characterizations

The samples were investigated using a VERTEX 80/Raman II fourier transform infrared spectroscopy (FTIR) spectrometer (bruker) unit with the range from 500 to 4000 cm^{-1} and ^1H nuclear magnetic resonance (NMR) measured in D_2O using a MHz spectrometer (Bruker). For morphology test, samples were prepared and measured according to Refs [31, 32] introducing transmission electron microscope (TEM) (JEM-1400 Plus) analysis of polymer conjugation and micelle aggregates with metal complex drugs in detail. The sample was negatively stained with a droplet of phosphotungstic acid and fixed on copper grids for 30 s before it bloted up with filter paper. Dynamic light scattering (DLS) was used to determine the hydrodynamic diameter of PEC-DO and PEC-DO + Ru conjugates on a Malvern Zetasizer NanoS instrument with a 4 mW He-Ne 633 nm laser module. The hydrodynamic radius was calculated from the Stokes–Einstein equation [33]. The UV–vis absorption measurements were taken at room temperature using a SPECORD S600 spectrophotometer (Jena, Jena, Germany). Fluorescence measurements were performed on a LS-50B spectrofluorometer (Perkin Elmer). X-ray diffraction (XRD) patterns of the samples were recorded on an X-ray diffract meter (D8 ADVANCE) at a voltage of 40 kV and a current of 40 mA using Cu K_α radiation. The scanning scope of 2θ was ranged from 10 to 50° at ambient temperature.

2.5. DO content measurement

The DO content of PEC–DO conjugates was obtained by measuring the absorbance at 280 nm. The solubility of PEC–DO conjugates in water was measured as follows. Firstly, 10 mg of PEC–DO conjugates was added to 1 mL of water and the mixture stirred quickly to dissolve the sample. Secondly, the suspension of PEC–DO conjugates was centrifuged at 12000 rpm for 5 min. The supernatant was diluted and the absorbance at 280 nm was measured.

2.6. Determination of antioxidant activity of PEC-DO conjugates

The ABTS radical cations clearance test was used to determine the antioxidant properties of DO, Ru complex, and PEC-DO [34]. ABTS was dissolved in water to a 7 mM (about 3.84 mg/mL) concentration. ABTS radical cations ($ABTS^{\cdot+}$) was produced by reacting ABTS stock solution with 2.45 mM $K_2S_2O_8$ (final concentration about 0.662 mg/mL) and allowing the mixture to stand in the dark at room temperature for 12–16 h before use. The ABTS radical solution was diluted 25 times and stored away from light until the absorbance at 734 nm was about 1.5. 160 μM DO (or Ru complex) solution was prepared for use. The first set of experiments: The eight different concentrations of DO (or Ru complex) (2 mL: 0, 20, 40, 60, 80, 100, 120, 140, 160 μM) were loaded into 8 centrifuge tubes (5 mL), respectively, those containing 2 mL ABTS cationic stock solution. The second set of experiments was the same as the first set of methods in which the concentration of PEC-DO was reported in terms of the amount of DO therein. The absorbance of the mixed solution at 734 nm was measured after mixing for five minutes. The ABTS radical scavenging activity of the sample was calculated as.

$$\text{Inhibition}\ (\%) = (1 - A_{sample}/A_{blank}) \times 100\% \quad (1)$$

where A_{blank} is the absorbance of the blank and A_{sample} is the absorbance of the mixed solution. The inhibition percentage increases with antioxidant activity.

The DPPH free radical (1,1-diphenyl-2-trinitrophenylhydrazine) was used as a radical scavenging assay to determine the antioxidant properties of PEC-DO [35]. DPPH stock solution (about 0.05 mg/mL) was prepared in methanol. 160 μM DO (or Ru complex) solution was prepared for use. The first set of experiments: The eight different concentrations of DO (or Ru complex) (2 mL: 0, 20, 40, 60, 80, 100, 120, 140, 160 μM) were loaded into 8 centrifuge tubes (5 mL), respectively, those containing 2 mL ABTS cationic stock solution. The second set of experiments was the same as the first set of method in which the concentration of PEC-DO was reported in terms of the amount of DO therein. The absorbance of the mixed solution at 517 nm was measured after mixing for five minutes. The ABTS radical scavenging activity of the sample was calculated as.

$$\text{Inhibition}\ (\%) = (1 - A_{sample}/A_{blank}) \times 100\% \quad (2)$$

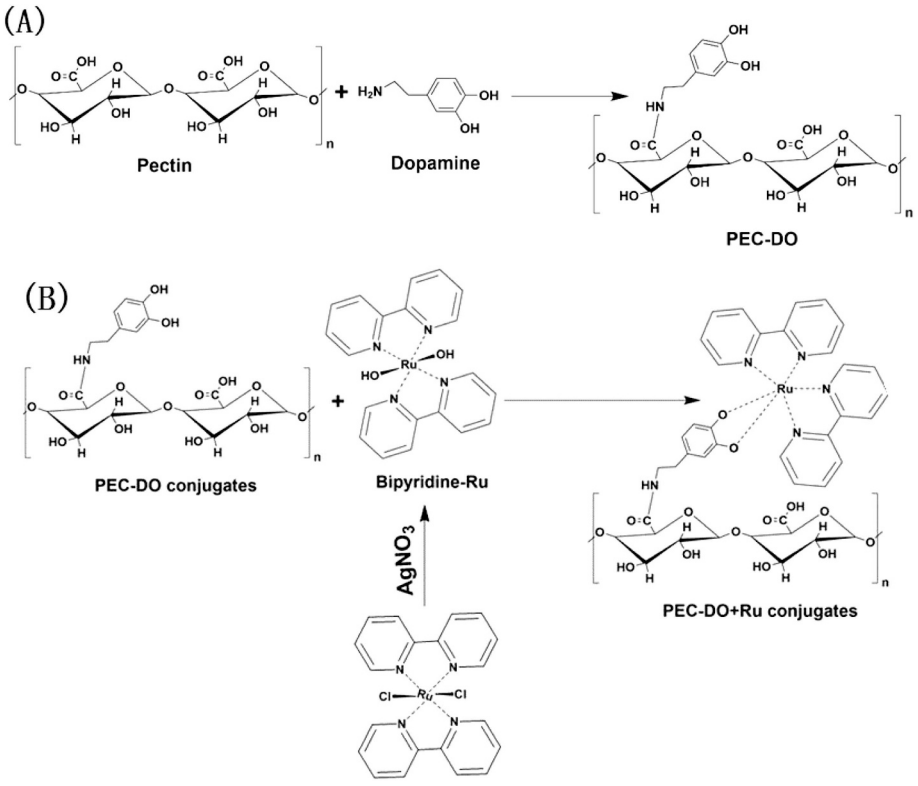

Fig. 1. The synthetic routes of PEC-DO(A) and PEC-DO + Ru conjugates (B).

where A_{blank} is the absorbance of the blank and A_{sample} is the absorbance of the mixed solution. The inhibition percentage increases with antioxidant activity.

2.7. Determination of the content of cis-Bis(2,2′-dipyridyl) ruthenium (II) chloride in the sample

The bis(2,2′-dipyridyl) ruthenium (II) chloride was chosen to prepare PEC-DO + Ru conjugates. The amount of bis(2,2′-dipyridyl) ruthenium (II) chloride in PEC-DO + Ru conjugates was determined using a standard curve method. Standard curve for bis(2,2′-dipyridyl) ruthenium dichloride (II): different concentrations of bis(2,2′-dipyridyl) ruthenium dichloride (II) were prepared in PBS buffer, respectively. The concentration range was 5–35 μg/mL. The absorption curve of bis (2,2′-dipyridyl) ruthenium dichloride (II) was measured by a UV–vis spectrophotometer, and the absorbance at 490 nm was taken. Taking the concentration of bis(2,2′-dipyridyl) ruthenium dichloride (II) as the abscissa and the absorbance as the ordinate, do the bis(2,2′-dipyridyl) ruthenium dichloride (II) to make the concentration of the standard curve.

PEC-DO + Ru conjugates in PBS buffer were weighed and prepared in a 0.5 mg/mL solution and its absorbance at 490 nm was determined. The amount of bis(2,2′-bipyridinyl) ruthenium dichloride (II) in PEC-DO + Ru conjugates was calculated from the standard curve.

2.8. The coordination ratio of cis-Bis(2,2′-dipyridyl) ruthenium (II) chloride to PEC-DO

The known concentration of PEC-DO solution was configured. According to the content of DO in PEC-DO conjugates, the molar amount of DO was calculated in the solution. 3 mL of PEC-DO solution was pipetted into the fluorescence cuvette. A solution of bis(2,2′-dipyridyl) ruthenium (II) chloride of known concentration was prepared, and add 10 μL of Ru complex to the PEC-DO solution by using a micropipettes in sequence, and the final molar amount of the bis (2,2′-dipyridyl) ruthenium (II) chloride in the mixed solution was 0, 0.5, 1.0, 1.5, 2.0, 2.5 times as much as the molar amount of DO. The sample was mixed uniformly, and the fluorescence emission spectra was measured with λ_{ex} = 280 nm after standing for 30 min. The fluorescence intensity is plotted on the ordinate and the molar ratio of bis(2,2′-dipyridyl) ruthenium (II) chloride to DO in the solution is plotted as the abscissa, fitting curve to obtain the coordination ratio of bis(2,2′-dipyridyl) ruthenium (II) chloride to dopamine.

2.9. Rheological measurements

Rheological measurements investigated using a TA Instruments DHR-1 Rheometer equipped with 40 mm aluminum plate geometry at a gap 53 μm and covered with a moisture trap. The samples in water were performed at concentration 2% w/v. The rheological results were obtained and analyzed using the TA rheometer Data Analysis software. The steady shear measurements were carried out to obtain the apparent viscosity of the samples at concentration at 2% w/v at 20 °C with the shear rate from 0 to 1000 1/s. Strain sweeps were run at 1 Hz and 0.1–1000% strain at 20 °C. Frequency sweeps were run at 2% strain and 0.001–5 Hz at 20 °C [36].

2.10. Cytotoxicity studies

Herein, Cell viability was tested by 3-(4,5-dimethylthiazol-2-yl)-2,5-diphenyltetrazolium bromide (MTT) colorimetric assay in order to evaluate the cytotoxicity of nano-conjugates against human ovarian cancer cell line Skov3, human renal cell adenocarcinoma cell line 786-O, human breast adenocarcinoma cell line MCF-7, human cervical cancer cell line HeLa, and human normal renal epithelial cell line 293A [37,38]. The cells were seeded into 96-well plates with a density of 1×10^4 cells per well for 24 h, and then different concentrations of Ru complex, PEC-DO, and PEC-DO + Ru conjugates were added to the cells and incubated for 48 h, respectively. After that, the culture medium was removed and the MTT solution (5 mg/mL) was added to the cells and

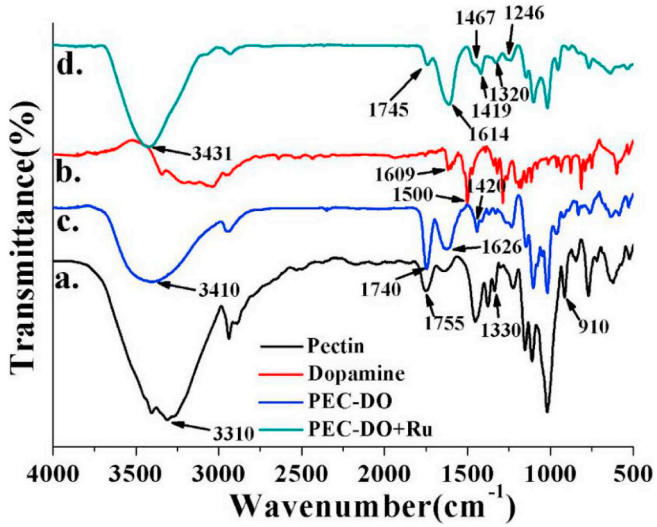

Fig. 2. FTIR spectra of (a) PEC, (b) DO, (c) PEC-DO, and (d) PEC-DO + Ru conjugates.

incubated for a further 4 h. The inhibition concentrate ion IC_{50} value expresses the concentration of Ru complex, PEC-DO conjugates, and PEC-DO + Ru conjugates required to result in 50.0% cell death, determined by the average of three duplicatem experimental results.

3. Results and discussion

3.1. FTIR spectral analysis

The fourier transform infrared spectroscopy (FTIR) spectra of pectin, DO, PEC-DO conjugates, and PEC-DO + Ru conjugates were measured in KBr disc. The results were illustrated in Fig. 2. Compared the FTIR spectra of PEC and DO, it was found that the characteristic absorption bands of the FTIR spectra at 1626 and 1420 cm^{-1} could be attributed to the bending vibration absorption of the N—H bond in the amide bond. The absence of the peak at 1330 cm^{-1} due to C—O bond and 910 cm^{-1} due to O—H, and the appearance of a new absorption at 1740 cm^{-1} indicated that the reaction occurred at the carboxyl group in PEC and PEC-DO was successfully synthesized. Based on the PEC-DO and PEC-DO + Ru conjugates spectral results, it was found that the peak of the −C═N bond in the pyridine ring appeared at 1614 cm^{-1} in the infrared spectrum of PEC-DO + Ru conjugates. PEC-DO showed a broad absorption peak of O—H bond and N—H bond stretching vibration at 3410 cm^{-1}, while N—H stretching vibration peak of PEC-DO + Ru conjugates at 3431 cm^{-1} was obviously narrower than PEC-DO conjugates. Thus, it could be shown that the hydroxyl group on the DO in PEC-DO was successfully coordinated with the bis(2,2′-dipyridyl) ruthenium (II) chloride to obtain the target product PEC-DO + Ru conjugates.

3.2. ^1H NMR analysis

DO, PEC-DO conjugates, and PEC-DO + Ru conjugates were separately dissolved in D_2O and subjected to ^1H nuclear magnetic resonance NMR measurement to confirm the structures of PEC-DO and PEC-DO + Ru conjugates. The ^1H NMR of DO was shown in the inset of Fig. 3(A). DO has an aromatic proton peak between 6.79 and 6.62 ppm and a proton peak on the alkyl chain between 3.12 and 2.73 ppm. In the ^1H NMR chart of PEC-DO (Fig. 3A), there are proton peaks between 5.50 and 3.50 ppm on the pectin backbone and aromatic proton peaks on DO in PEC-DO conjugates at 6.80, 6.74, and 6.65 ppm. The above results indicated that PEC was successfully modified by DO. In the ^1H NMR chart of PEC-DO + Ru conjugates (Fig. 3B), they have aromatic

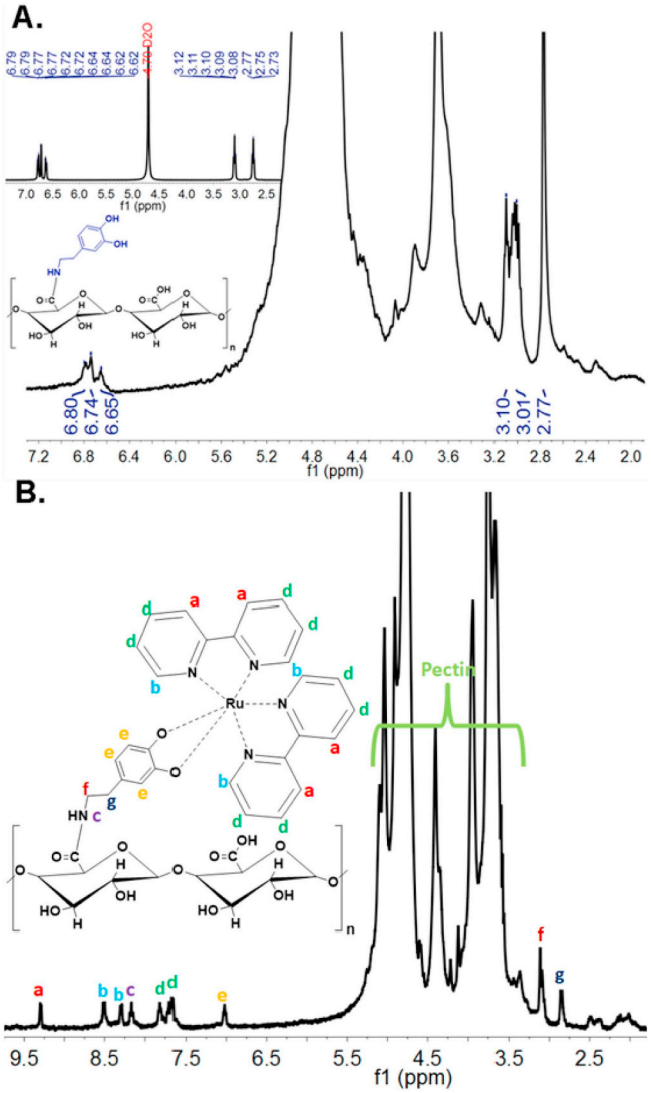

Fig. 3. ^1H NMR spectra of (A) PEC-DO and (B) PEC-DO + Ru conjugates, the inset of Panel (A) showed the ^1H NMR spectrum of DO.

peaks corresponding to the pyridine ring at 9.30, 8.52, 8.29, 7.82, and 7.67 ppm, and correspond to -NH- in DO at 8.17 ppm. The proton peak at 7.02 ppm corresponds to the aromatic proton peak on DO in PEC-DO + Ru conjugates, and there are proton peaks on the alkyl chain on DO in PEC-DO + Ru conjugates at 3.11, 2.84 ppm. The δ between 5.50 and 3.50 ppm is the proton peak on the PEC skeleton of PEC-DO + Ru conjugates. The above results indicated that PEC-DO conjugates have been successfully coordinated by the *cis*-bis(2,2′-dipyridyl) ruthenium (II) dichloride.

3.3. DO grafting amount and solubility in the sample

According to the method described in the experiment, the standard curve of PEC-DO conjugates in PBS solution was first plotted to obtain the standard curve equation,

$$A = 0.0138C + 0.0176 \ (R^2 = 0.9998) \quad (3)$$

The absorbance of a known concentration of PEC-DO conjugates solution was measured and taken into the standard equation to calculate a dopamine content of approximately 4.5 mg/100 mg. Through the preparation of supersaturated PEC-DO conjugates solution, after high-speed centrifugation, the supernatant was diluted to measure the absorbance. Finally, based on the content of DO, the solubility of PEC-DO

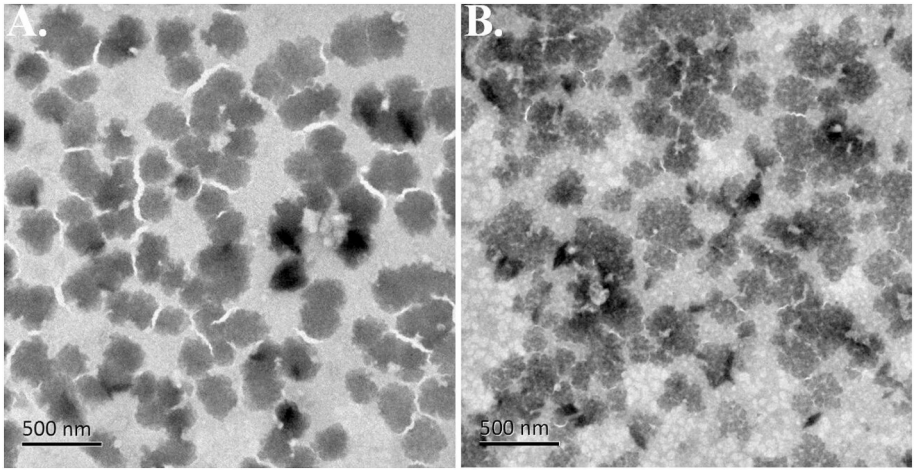

Fig. 4. The morphology of (A) PEC-DO and (B) PEC-DO + Ru conjugates.

conjugates was calculated to be approximately 8.2 mg/mL.

3.4. TEM and DLS analysis

TEM images of PEC-DO and PEC-DO + Ru conjugates were obtained, as shown in Fig. 4. It can be seen from the figure that PEC-DO self-aggregates into relatively regular nanoparticles of approximately 200 nm after spreading the sample solution on copper grid and draining the excess using filter paper after 60 s. When ruthenium complex is coordinated with PEC-DO, the spherical particles became smaller and partly damaged, which may be caused by the inhomogeneous coordination of *cis*-bis(2,2′-dipyridyl) ruthenium (II) dichloride. The strong bonding between the metal and its ligands changed the state of PEC-DO aggregation. In addition, the removal of the solvent from PEC-DO and PEC-DO + Ru conjugates solution result in appearing flat and quite ragged.

Herein, DLS was used to analysis the size of PEC-DO and PEC-DO + Ru conjugates self-aggregates in solution. The results were shown in Fig. 5(A, B). The diameter of PEC-DO and PEC-DO + Ru conjugates range from 70 to 200 nm and from 80 to 300, suggesting that the conjugates were formed through self-assembly in the aqueous solution. The range of different size distribution of PEC-DO + Ru conjugates could have been caused by the coordination of Ru complex with PEC-DO. The different ligands on PEC-DO and PEC-DO + Ru conjugates partly impact the binding force between molecules that changed the state of aggregations in solution.

3.5. Powder X-ray diffractometry

X-ray powder diffraction patterns of PEC, PEC-DO conjugates, PEC-DO + Ru conjugates, and Ru complex were shown in Fig. 6. It can be seen from Fig. 6 that PEC and Ru complex have sharper crystallization peaks, but the crystalline of PEC-DO conjugates and PEC-DO + Ru conjugates obtained after the reaction is not high, and there are no sharp crystallization peaks. This indicates that the modified PEC-DO and PEC-DO + Ru conjugates lose their original crystal structure due to the non-uniform grafting of DO. The PEC-DO and PEC-DO + Ru conjugates were considerably more amorphous than PEC and the structure of pectin was greatly perturbed by anchoring DO and Ru complex to

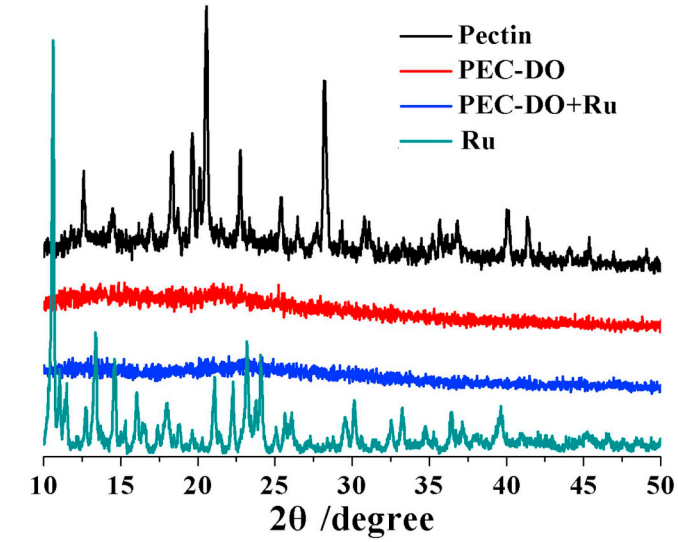

Fig. 6. XRD of samples: (a) PEC, (b) PEC-DO, (c) PEC-DO + Ru and (d) Ru complex.

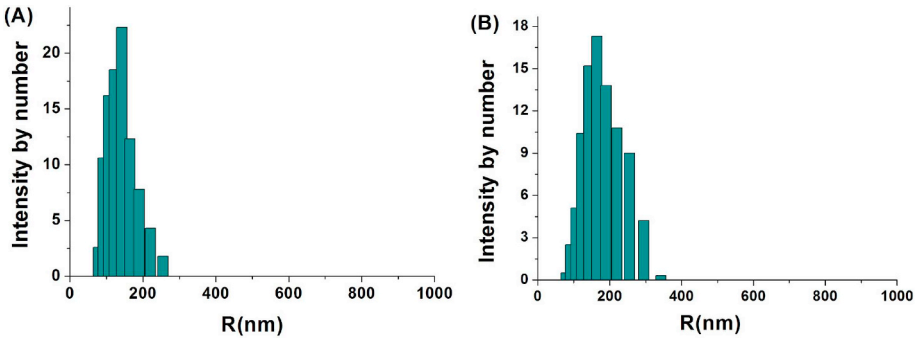

Fig. 5. DLS pattern of PEC-DO(A) and PEC-DO + Ru(B). Spectra were recorded at room temperature; 3 mg/mL; the solutions were not filtered before analysis.

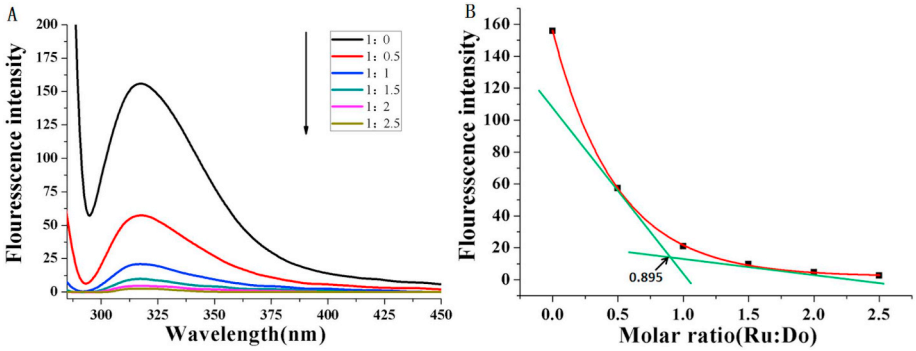

Fig. 7. (A) The fluorescence curve of PEC-DO in the presence of different concentration of Ru complex, [DO in PEC-DO] = 10 μM, in water. [Ru complex] (from up to down), 0 μM, 0.5 μM, 10 μM, 15 μM 20 μM, 25 μM; (B) The fitting curve of fluorescence intensity and mole ratio of Ru:Do.

their backbone [23].

3.6. Content of coordination cis-bis(2,2′-dipyridyl) hafnium dichloride (II) in the sample

Through the experiment, the standard curve of Ru complex in PBS solution was first plotted to obtained the standard equation,

$$A = 0.01062C + 0.00307 \ (R^2 = 0.9991) \quad (4)$$

The experimentally prepared PEC-DO + Ru conjugates were formulated into a 0.5 mg/mL solution and its absorbance at 480 nm was measured. According to the standard curve, the weight amount of Ru complex in PEC-DO + Ru conjugates was calculated as 21.41%.

3.7. The coordination ratio of cis-Bis(2,2′-dipyridyl) ruthenium (II) chloride to PEC-DO

The fluorescence emission of PEC-DO conjugates was obtained with excitation wavelength 280 nm (Fig. 7). The fluorescence intensity of emission wavelength at 317 nm was used to make a plot of fluorescence intensity/M amount of Ru:DO. The curve was obtained by fitting and the inflection point of the curve was obtained. The coordination molar ratio of *cis*-bis(2,2′-dipyridyl) ruthenium (II) dichloride to DO, and its value was 0.895:1, indicating that PEC-DO conjugates and Ru complex can be successfully coordinated, which makes PEC-DO conjugates a new type of drug delivery system and offers the possibility of transporting metal drugs. The application of PEC-DO + Ru conjugates in the treatment of cancer cells needs further study.

3.8. The rheological analysis

The rheological and viscoelastic behavior of polysaccharide-metal complex was studied from the structure and function analysis. The rheological properties are one of the most important functional properties of polysaccharides [39,40]. Fig. 8 showed the stead shear flow curves of PEC, PEC-DO conjugates, and PEC-DO + Ru conjugates. It can be found that the viscosity of the samples decreased as shear rate increased, indicating the shear-thinning behavior of PEC, PEC-DO conjugates, and PEC-DO + Ru conjugates. They have the pseudoplastic behavior of the non-Newtonian behaviors. In addition, the values of viscosity of PEC-DO conjugates, and PEC-DO + Ru conjugates are bigger than that of PEC, suggesting that the modification of PEC by DO and Ru complex did obviously decrease the apparent viscosity of polysaccharides. The reason for this situation should be that the modification of PEC by using DO and Ru complex weak the intermolecular forces and result in the intermolecular partial unwrapping of PEC, and make it easier for large molecules to move.

To characterize the dynamic rheological properties of PEC, PEC-DO, and PEC-DO + Ru conjugates, the strain and frequency dependence of

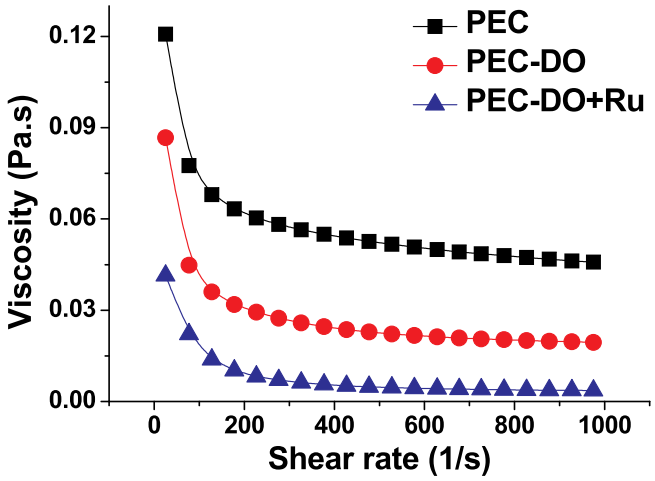

Fig. 8. Stead shear flow curves of PEC, PEC-DO, and PEC-DO + Ru, c(PEC) = c (PEC-DO) = c(PEC-DO + Ru) = 2% w/v.

the storage modulus (G′) and loss modulus (G″) at 25 °C for 2% (w/v) of the samples dispersion were measured and shown in Fig. 9(A, B). Fig. 9(A) showed that a strain sweep was performed at constant frequency (1 Hz), it was found that the order of the value changes of G′ was G′(PEC-DO + Ru) > G′(PEC) > G′(PEC-DO), indicating a higher rigidity of the PEC-DO + Ru conjugates system. In addition, both G′ and G″ of PEC-DO + Ru conjugates decreased faster than those of PEC and PEC-DO conjugates, suggesting that PEC-DO + Ru conjugates system cannot withstand as much strain as the PEC and PEC-DO systems before it is structurally disrupted [36].

The frequency dependence of the storage and loss shear moduli (G′ and G″) is shown in Fig. 9(B), which showed the viscoelastic behavior of PEC, PEC-DO conjugates, and PEC-DO + Ru conjugates. As the results showed, PEC-DO + Ru conjugates exhibited the typical viscoelastic behavior of transient networks [41] as G′ is higher than G″ at high frequencies but decreased below G″ at lower frequencies. The gel strength of PEC-DO + Ru conjugates was better than those of PEC and PEC-DO. Seen from the results, it was found a common point that all the values of G″ are larger than those of G′, indicating that the viscous behaviors of PEC, PEC-DO conjugates and PEC-DO + Ru conjugates solutions are greater than their elastic behaviors, respectively [42]. In addition, the modification of PEC with DO and Ru complex obviously changed the polymer network of PEC. These above conclusions are very consistent with the XRD results.

3.9. Antioxidant activity evaluation

DO, as a natural polyphenol, has its own good antioxidant activity.

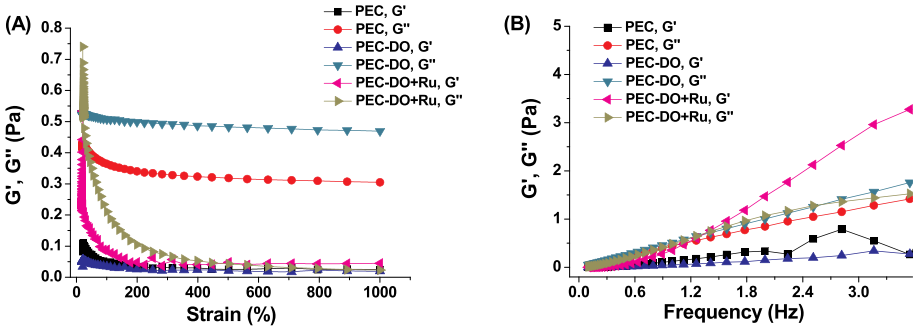

Fig. 9. Rheological properties of PEC, PEC-DO, and PEC-DO + Ru: (A) strain sweep at constant 1 Hz, (B) frequency sweep at constant 2% strain, c(PEC) = c(PEC-DO) = c(PEC-DO + Ru) = 2% w/v.

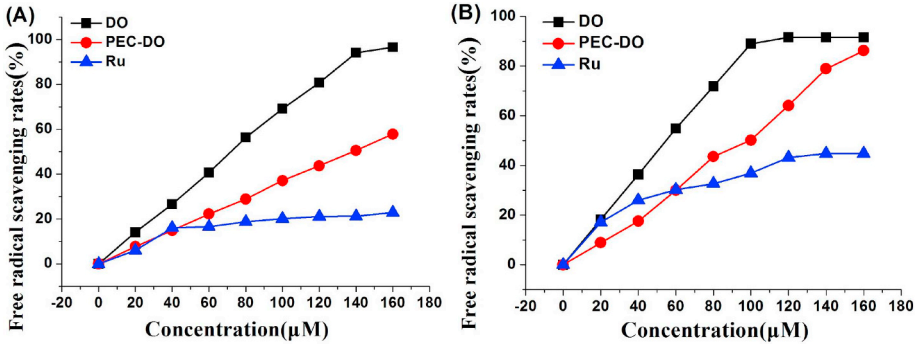

Fig. 10. The free radical scavenging rate of DO, PEC-DO, and Ru complex. (A, ABTS free radical; B, DPPH radical).

In order to study whether DO-modified PEC can retain good antioxidant activity, we designed experiments and measured the antioxidant activity of DO, PEC-DO conjugates, and Ru complex. The concentration of DO grafted in the product PEC-DO conjugates is shown in Fig. 10. Fig. 10(A) shows the removal rate of ABTS free radicals, and Fig. 10(B) shows the removal rate of DPPH free radicals. As can be seen from Fig. 10, DO have better scavenging effecting on both ABTS and DPPH radicals than those of PEC-DO conjugates and Ru complex. The order of antioxidant of them was DO > PEC-DO > Ru complex. When DO is grafted onto PEC, its clearance rate for these two kinds of free radicals is lower than that of itself. However, DO retains its antioxidant activity and PEC-DO also has good anti-oxidant activity.

3.10. Anti-cancer activity of PEC-DO + Ru conjugates

Herein, the in vitro cytotoxicity of the Ru complex, DO, PEC-DO conjugates, or PEC-DO + Ru conjugates was evaluated in Skov3, 786-O, MCF-7, HeLa, HepG2, and 293A cells using MTT assay in order to analyze the further applications of the nanoconjugates in biomedical fields. The IC_{50} value of Skov3, 786-O, MCF-7, HeLa, HepG2, and 293A treated with free Ru complex, DO, PEC-DO conjugates, and PEC-DO + Ru conjugates were shown in Fig. 11. Firstly, as shown in Fig. 11, the IC_{50} value of PEC-DO conjugates against human normal renal epithelial cell line 293A were (634.10 ± 9.78) μmol/L, exhibiting good biocompatibility and low toxicity to human normal cell. And in contrast, PEC-DO exhibited higher toxicity against Skov3 (115.76 ± 0.04) μmol/L than 786-O (240.58 ± 3.91) μmol/L, MCF-7 (308.64 ± 8.89) μmol/L and HeLa (912.2 ± 46.99) μmol/L. Secondly, Fig. 11 showed the IC_{50} value of Skov3, 786-O, MCF-7, HeLa, HepG2, and 293A treated with free Ru complex were (25.92 ± 0.03) μmol/L, (47.00 ± 0.03) μmol/L, (93.58 ± 1.11) μmol/L, (137.73 ± 0.07) μmol/L, (40.16 ± 0.73) μmol/L, and (225.54 ± 2.05) μmol/L, respectively. The IC_{50} value of Skov3, 786-O, MCF-7, HeLa, HepG2, and 293A treated with PEC-DO + Ru conjugates were (228.39 ± 1.56) μmol/L, (45.30 ± 0.05) μmol/L, (228.39 ± 1.56) μmol/L, (351.04 ± 18.23)

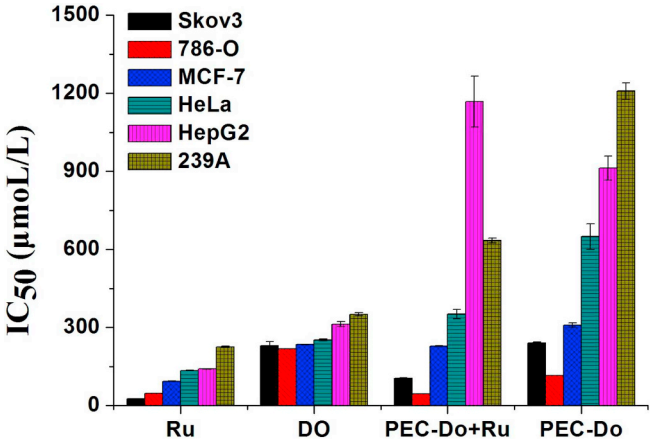

Fig. 11. IC_{50} value of Skov3, 786-O, MCF-7, HeLa, HepG2, and 293A treated with free Ru complex, DO, PEC-DO, and PEC-DO + Ru conjugates.

μmol/L, (1167.99 ± 98.33) μmol/L, and (634.10 ± 9.78) μmol/L, respectively. As the results showed, the conjugates exhibited obviously lower toxicity against human normal renal epithelial cell line 293A than that of Ru complex, indicating that PEC-DO conjugates may decrease the toxicity effect of Ru complex in human body [43]. In addition, the conjugates also exhibit lower toxicity against Skov3, MCF-7, HeLa, and HepG2 except 786-O than those of Ru complex, implying that PEC-DO not only has good biocompatibility, but also increase the targeting of cancer therapy, since PEC-DO + Ru conjugates always continue to have higher toxicity against 786-O, which has a certain relationship with the anticancer activity of PEC-DO. At present, PEC based conjugates have been studied to improve the efficacy of free anticancer drugs in vivo [44,45]. The results from Zhang et al. showed that PEC can inhibits tumor growth and metastasis, induce apoptosis, and modulate immunological responses with a high bioavailability and bioactivity [46]. Such as desirable enhanced permeability and retention

effect, biodegradable, and either eliminate or minimize toxicity of PEC nano-conjugates possible effect Ru complex anticancer activity [14]. In addition, the IC_{50} value of Skov3, 786-O, MCF-7, HeLa, HepG2, and 293A treated with DO were (229.18 ± 15.59) μmol/L, (217.78 ± 0.32) μmol/L, (234.92 ± 0.84) μmol/L, (251.79 ± 3.63) μmol/L, (313.12 ± 8.91) μmol/L, and (350.77 ± 5.84) μmol/L, respectively, indicating that DO did not show higher toxicity against above five cells. Therefore, dopamine plays an important role in carrying ruthenium complex by the coordination. In a word, The PEC-DO + Ru conjugates may be applied in treating human renal clear cell carcinoma without toxic and side effects on the human normal renal epithelial cell.

4. Conclusions

The obtained results from this work revealed that PEC-DO + Ru conjugates were successfully designed by modifying PEC with DO to link ruthenium complex. Nano-conjugates of PEC bearing anchored ruthenium complexes ca. 200 nm in size was revealed by TEM. The modification of PEC by DO and Ru complex not only changed the amorphous network of PEC, but also affected the viscosity and viscoelastic behavior of it. It is important that PEC-DO conjugates retain the free radical scavenging ability of DO and has good biocompatibility. In addition, PEC-DO + Ru conjugates exhibit higher toxicity against 786-O cells. These findings show that PEC-DO + Ru conjugates increase the perspectives for development and medical applications of new anticancer metal-based drugs.

Abbreviations

293A	human normal renal epithelial cell line
786-O	human renal cell adenocarcinoma cell line
ABTS	2,2′-Azino-di-[3-ethylbenzthiazoline sulfonate]
DLS	Dynamic light scattering
DMF	*N*,*N*-dimethyllformamide
DO	dopamine
DPPH	1,1-Diphenyl-2-picrylhydrazyl radical 2,2-Diphenyl-1-(2,4,6-trinitrophenyl) hydrazyl
EDC	*N*-(3-Dimethylaminopropyl)-*N*′-ethylcarbodiimide hydrochloride
FTIR	fourier transform infrared spectroscopy
G′	storage modulus
G″	loss modulus
HeLa	human cervical cancer cell line
MES	2-(*N*-morpholine)ethanesulfonic acid
MCF-7	human breast adenocarcinoma cell line
MTT	3-(4,5-dimethylthiazol-2-yl)-2,5-diphenyltetrazolium bromide
NHS	*N*-Hydroxy-succinimide
NMR	nuclear magnetic resonance
PEC	pectin
PEC-DO	pectin-dopamine
PEC-DO + Ru	pectin-dopamine Ru complex
PMCs	polymer-metal complexes
Ru	*cis*-Bis(2,2′-Dipyridyl) ruthenium(II) dichloride
RuPMc	ruthenium cyclopentadienyl complex
Skov3	human ovarian cancer cell line
TEM	transmission electron microscope
XRD	X-ray diffraction

Acknowledgements

This work was supported by the National Natural Science Foundation of China (Grant No. 21571154, 31600722), the Natural Science Foundation of Jiangsu Province (Grant No. BK20161315, BK20151296), the “Six Talent Peaks Project” in Jiangsu Province, the Jiangsu Fundament of “Qinglan Project” and “333 Project”.

References

[1] H. Gheybi, H. Niknejad, A.A. Entezami, Des. Monomers Polym. 17 (2014) 334–344.
[2] Z. Zhang, Y. Li, J. Wan, P. Long, J. Guo, G. Chen, C. Wang, Polym. Chem. 8 (2017) 2410–2422.
[3] A. Valente, M.H. Garcia, F. Marques, Y. Miao, C. Rousseau, P. Zinck, J. Inorg. Biochem. 127 (2013) 79–81.
[4] W. Sun, X. Zeng, S. Wu, Dalton Trans. 47 (2018) 283–286.
[5] H.B. Ruttala, T. Ramasamy, B. Gupta, H.G. Choi, C.S. Yong, J.O. Kim, Carbohydr. Polym. 173 (2017) 57–66.
[6] F. Ji, J. Li, Z. Qin, B. Yang, E. Zhang, D. Dong, J. Wang, Y. Wen, L. Tian, F. Yao, Carbohydr. Polym. 177 (2017) 86–96.
[7] M. Libera, P. Formanek, L. Schellkopf, B. Trzebicka, A. Dworak, M. Stamm, J. Polym. Sci. A 52 (2014) 3488–3497.
[8] Y. Zhang, T. Sun, C. Jiang, Acta Pharm. Sin. B 8 (2018) 34–50.
[9] Y. Huang, Y. He, Z. Huang, Y. Jiang, W. Chu, X. Sun, L. Huang, C. Zhao, Nanoscale 9 (2017) 10002–10019.
[10] X. Li, Y. Zhang, H. Chen, J. Sun, F. Feng, ACS Appl. Mater. Interfaces 8 (2016) 22756–22761.
[11] Z. Liu, Y. Jiao, Y. Wang, C. Zhou, Z. Zhang, Adv. Drug Deliv. Rev. 60 (2008) 1650–1662.
[12] J. Wang, G. Zuo, J. Li, T. Guan, C. Li, R. Jiang, B. Xie, X. Lin, F. Li, Y. Wang, D. Chen, Int. J. Biol. Macromol. 46 (2010) 89–95.
[13] K. Cheewatanakornkool, S. Niratisai, S. Manchun, C.R. Dass, P. Sriamornsak, Carbohydr. Polym. 174 (2017) 493–506.
[14] Y. Liu, K. Liu, X. Li, S. Xiao, D. Zheng, P. Zhu, C. Li, J. Liu, J. He, J. Lei, L. Wang, Mater. Sci. Eng. C 86 (2018) 28–41.
[15] A.K. Verma, K. Sachin, Curr. Drug Deliv. 5 (2008) 120–126.
[16] Z. Zhang, J. Chen, J. Yu, Q. Zhao, C. Cao, J. Shen, D. Shi, Chin. J. Appl. Chem. 35 (2018) 665–673.
[17] X. Wang, Z. Jiang, J. Shi, C. Zhang, W. Zhang, H. Wu, Ind. Eng. Chem. Res. 52 (2013) 14828–14836.
[18] H.K. Liu, S.J. Berners-Price, F.Y. Wang, J.A. Parkinson, J.J. Xu, J. Bella, P.J. Sadler, Angew. Chem. Int. Ed. 45 (2006) 8153–8156.
[19] H.K. Liu, J.A. Parkinson, J. Bella, F.Y. Wang, P.J. Sadler, Chem. Sci. 1 (2010) 258–270.
[21] Q. Wu, L.Y. Liu, S. Li, F.X. Wang, J. Li, Y. Qian, Z. Su, Z.W. Mao, Peter J. Sadler, H.K. Liu, J. Inorg. Biochem. 189 (2018) 30–39.
[22] F. Schmitt, J. Kasparkova, V. Brabec, G. Begemann, R. Schobert, B. Biersack, J. Inorg. Biochem. 184 (2018) 69–78.
[23] Y.Q. Wang, A. Pitto-Barry, A. Habtemariam, I. Romero-Canelon, P.J. Sadler, N.P.E. Barry, Inorg. Chem. Front. 3 (2016) 1058–1064.
[24] E.M. Linares, A. Formiga, L.T. Kubota, F. Galembeck, S. Thalhammer, J. Mater. Chem. B 1 (2013) 2236–2244.
[25] S. Michlewska, M. Ionov, M. Maroto-Díaz, A. Szwed, A. Ihnatsyeu-Kachan, S. Loznikova, D. Shcharbin, M. Maly, R.G. Ramirez, F.J. Mata, M. Bryszewska, J. Inorg. Biochem. 181 (2018) 18–27.
[26] B.M. Blunden, A. Rawal, H. Lu, M.H. Stenzel, Macromolecules 47 (2014) 1646–1655.
[28] V. Nandakumar, V. Vettriselvi, M. Doble, RSC Adv. 4 (2014) 11438–11443.
[29] W. Sun, M. Parowatkin, W. Steffen, H.J. Butt, V. Mailänder, S. Wu, Adv. Healthc. Mater. 5 (2016) 467–473.
[30] W.J. Rieter, K.M. Pott, K.M.L. Taylor, W. Lin, J. Am. Chem. Soc. 130 (2008) 11584–11585.
[31] V.T. Huynh, J.Y. Quek, P.L. Souza, M.H. Stenzel, Biomacromolecules 13 (2012) 1010–1023.
[32] V.T. Huynh, G. Chen, P. Souza, M.H. Stenzel, Biomacromolecules 12 (2011) 1738–1752.
[33] J.T. Edward, J. Chem. Educ. 47 (1970) 261.
[34] R. Re, N. Pllegrini, A. Poteggente, A. Pnnala, M. Yang, C. Riceevans, Free Radic. Biol. Med. 26 (1999) 1231–1237.
[35] B. Li, S. Konecke, L.A. Wegiel, L.S. Taylor, K.J. Edgar, Carbohydr. Polym. 98 (2013) 1108–1116.
[36] X. Zhang, R.M. Waymouth, J. Am. Chem. Soc. 139 (2017) 3822–3833.
[37] M.B. Hansen, S.E. Nielsen, K. Berg, J. Immunol. Methods 119 (1989) 203–210.
[38] F. Bai, J.J. Diao, Y. Wang, S.X. Sun, H.M. Zhang, Y.Y. Liu, Y.Q. Wang, J. Cao, J. Agric. Food Chem. 65 (2017) 6840–6847.
[39] H. Bao, S. You, L. Cao, R. Zhou, Q. Wang, S.W. C, Food Hydrocoll. 57 (2016) 36–37.
[40] M. Salehi, M. Tabarsa, M. Amraie, M. Anvari, M. Rezaei, B.M. Smith, Int. J. Biol. Macromol. 117 (2018) 294–300.
[41] C.J. Kloxin, C.N. Bowman, Chem. Soc. Rev. 42 (2013) 7161–7173.
[42] K. Nishinari, Colloid Polym. Sci. 275 (1997) 1093–1107.
[43] R.M.M. Oliveira, J.F.S. Daniel, R.M. Carlos, J. Mol. Struct. 1031 (2013) 269–274.
[44] S. Majzoob, F. Atyabi, F. Dorkoosh, K. Kafedjiiski, B. Loretz, A. Bernkopschnürch, J. Pharm. Pharmacol. 58 (2006) 1601–1610.
[45] G. Perera, J. Barthelmes, A. Bernkop-Schnürch, J. Control. Release 145 (2010) 240–246.
[46] W. Zhang, P. Xu, H. Zhang, Trends Food Sci. Technol. 44 (2015) 258–271.